Gain Apodization in Highly Doped, Distributed-Feedback (DFB) Fiber Lasers

Introduction

Fiber lasers have been the subject of much research over the past ten years. They can provide high reliability, fiber compatibility, high output power, good beam quality, narrow bandwidth, low phase noise, and low relative intensity noise (RIN).[1–4] These characteristics make them promising alternatives to solid-state and semiconductor lasers. Distributed-feedback (DFB) fiber lasers can be designed with a grating structure to provide high output power (up to 60 mW), single frequency,[5] single polarization,[6] and high optical signal-to-noise ratio (OSNR).[6] DFB fiber lasers have been widely used in sensing,[7] communication systems,[8–11] and high-precision spectroscopy,[12] all of which require single-mode, single-frequency lasers.

To obtain higher-power DFB fiber lasers, doping levels have been increased to allow more pump light to be absorbed with the doping densities of commercial Yb-doped fibers approaching $1 \times 10^{25}/\text{cm}^3$ (e.g., INO, Nufern). With the commercial availability of 500-mW pump lasers, the absorption transition easily becomes saturated. As the majority of the pump light is absorbed or converted into lasing photons, however, the remainder of the fiber is essentially unpumped. The transition length between the pumped and unpumped regions is given by the small-signal absorption, which is of the order of a millimeter or less. This gain apodization effect with pumped and unpumped sections of the DFB laser has so far been neglected.

In this article, the effects of gain apodization in DFB fiber lasers are investigated. In particular, the impact on threshold behavior is explored along with its effect on output power and mode discrimination. In the following sections (1) the conventional model based on coupled-wave equations is reviewed and applied to our case of fiber lasers; (2) the physics of gain apodization in DFB lasers is explored and compared to conventional configurations; (3) the impact of gain apodization on phase-shifted DFB fiber lasers is investigated; (4) lasing thresholds and the output power ratio from both ends of the fiber lasers are analyzed; and, finally, (5) techniques for using gain apodization as an optimization tool are discussed.

Coupled-Wave Matrix Model

Although DFB lasers are widely used for single-mode operation, in general their mode spectrum is more complicated. In a uniform index-coupled DFB fiber laser without phase shift or end mirrors, DFB lasers can operate in one of two degenerate longitudinal modes symmetrically located along the Bragg frequency of the grating. Nominally, only a single mode runs because of fabrication imperfections that cause slight asymmetry.

Coupled-mode theory[13,14] can be used to analyze the threshold behavior in simple DFB lasers. Figure 107.39 is a schematic of the coupling between forward and backward waves in waveguides induced by periodic modulation of the refractive index n. For a uniform fiber grating with uniform gain, the coupled-wave equations can be written as[15]

$$\begin{aligned} dE_A/dz &= \kappa \exp\left[i\left(2\Delta\beta z - \phi\right)\right]E_B + gE_A, \\ dE_B/dz &= \kappa \exp\left[-i\left(2\Delta\beta z - \phi\right)\right]E_A - gE_B, \end{aligned} \tag{1}$$

where E_A and E_B are the complex amplitudes of the forward and backward propagating waves, $\Delta\beta = \beta - m\pi/\Lambda$ is the propagation constant difference between the wave in the z direction and the m^{th} Bragg frequency of the grating ($m = 1$ for first-order gratings), ϕ is the wave phase at the position $z = 0$, κ is the coupling coefficient between the forward and

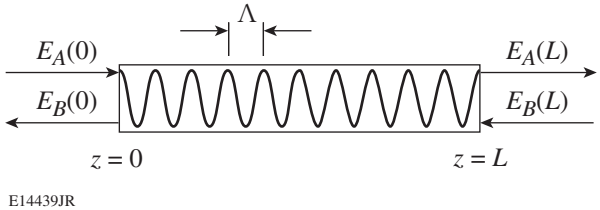

Figure 107.39
Schematic of coupled waves in periodic active waveguides.

backward waves in the grating, and g is the gain coefficient of the active medium collocated with the grating. In the absence of reflections from either side of the structures, Eq. (1) can be solved analytically.

To model a more complicated structure, e.g., where the gain is not constant along z, a matrix method[15,16] can be used to concatenate the solutions to Eq. (1). In this formalism, a nonuniform periodic structure is broken into segments of uniform period structures each with the solution

$$\begin{bmatrix} E_A(z_{j+1}) \\ E_B(z_{j+1}) \end{bmatrix} = \begin{pmatrix} F_{11}^j & F_{12}^j \\ F_{21}^j & F_{22}^j \end{pmatrix} \begin{bmatrix} E_A(z_j) \\ E_B(z_j) \end{bmatrix}, \tag{2}$$

where the matrix elements are the solutions to Eq. (1) given by

$$\begin{aligned} F_{11}^j &= \left[\cosh(\gamma_j L_j) + i\Delta\beta'_j\, L_j \sinh(\gamma_j L_j)/(\gamma_j L_j)\right] \\ &\quad \times \exp\left(i\beta_B^j L_j\right), \\ F_{12}^j &= -\kappa_j L_j \sinh(\gamma_j L_j)\exp\left[-i\left(\beta_B^j L_j + \phi_j\right)\right]/(\gamma_j L_j), \\ F_{21}^j &= -\kappa_j L_j \sinh(\gamma_j L_j)\exp\left[i\left(\beta_B^j L_j + \phi_j\right)\right]/(\gamma_j L_j), \\ F_{22}^j &= \left[\cosh(\gamma_j L_j) - i\Delta\beta'_j\, L_j \sinh(\gamma_j L_j)/(\gamma_j L_j)\right] \\ &\quad \times \exp\left[-i\left(\beta_B^j L_j\right)\right], \end{aligned} \tag{3}$$

and where $\Delta\beta'_j = \Delta\beta_j + ig_j$, $\gamma_j^2 = \kappa_j^2 - (\Delta\beta'_j)^2$, and $\beta_B^j = \pi/\Lambda_j$. With this formalism the active gratings can be split into N sections where the total matrix will be $F_t = F_N F_{N-1} \ldots F_2 F_1$. For a nonuniform DFB fiber laser, the coupling coefficient κ and gain coefficient g can change with the position z. For DFB fiber lasers without a phase shift, the phase terms in Eq. (3) can be written as $\phi^k = \phi^{k-1} + 2\beta_B^k L^{k-1}$, where k = 1,2,…N. For phase-shifted DFB fiber lasers, the phase terms in Eq. (3) can be written as $\phi^k = \phi^{k-1} + 2\beta_B^k L^{k-1} + \Delta\phi^k$, k = 1,2,…N. Adding the boundary conditions $E_A(0) = E_B(L) = 0$, the gain threshold condition can be obtained from the relation F_{t11} = 0 (Ref. 15). Nominally, this relation will produce a mode spectrum with different modes appearing at different frequencies $\Delta\beta$.

For high-power operation, it is desirable not only to have a low threshold but also to have most of the light coming out of only one side of the cavity. By using the total matrix F_t, the output power ratio from both ends of the fiber can be written as

$$\frac{P_1}{P_2} = \left|\frac{E_B(0)}{E_A(L)}\right|^2 = \left|F_{21}^2\right|, \tag{4}$$

where P_1/P_2 presents the ratio of the power coupling out at $z = 0$, as compared to $z = L$.

Gain-Apodization Physics

To understand the physics introduced by gain apodization, the formalism in the previous section is applied to three cases. In all cases, the grating strength κ and period Λ are kept constant and no phase shift will be included. The peak reflectivity of the grating is determined by $R = \tanh^2(\kappa L)$, and, so that the desired generality is not lost, typical values for κ and L are chosen. In the following sections, the coupling coefficient of the fiber grating is $\kappa = 1\ \text{cm}^{-1}$ and the grating lengths are 3 cm in most cases. Since the length under which the gain will drop from its maximum value to zero is less than 1 mm, the gain apodization along the z axis will be approximated by a step function. The gain-apodized DFB fiber laser is schematically shown in Fig. 107.40(a), where the L_1 section is highly doped with the uniform gain coefficient g and L_2 has no gain. This case will be compared to two other cases: The first, a DFB fiber laser of length L_1 and uniform gain but no unpumped section, is shown in Fig. 107.40(b). The second case, shown in

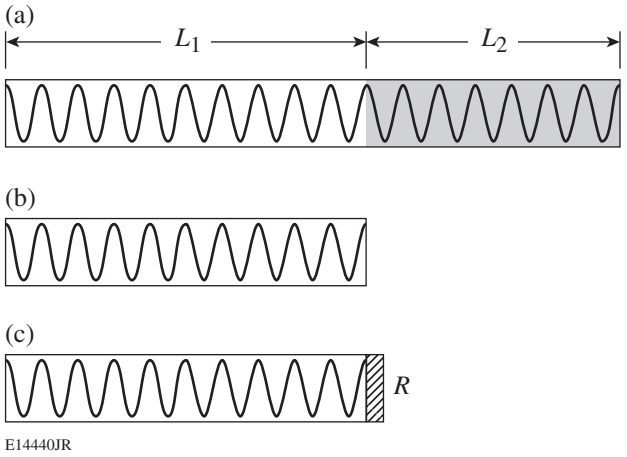

Figure 107.40
Schematic of the (a) gain-apodized DFB fiber laser, (b) uniform DFB fiber laser, and (c) uniform DFB fiber laser with end reflector $R_2 = \tanh^2(\kappa L_2)$. The shaded regions indicate sections with no gain.

Fig. 107.40(c), is the same laser as shown in Fig. 107.40(b) but with a reflector at the end of the cavity where the grating would be in the apodized case. The reflectivity value is chosen to be the peak reflectivity of the unpumped fiber grating of the case shown in Fig. 107.40(a), namely, $R_2 = \tanh^2(\kappa L_2)$. This value was chosen to directly compare to the apodized case shown in Fig. 107.40(a).

The gain thresholds for these cases where $L_1 = 2.5$ cm and $L_2 = 0.5$ cm are shown in Fig. 107.41. The horizontal axis is the normalized frequency $\Delta\beta L$ (where $L = L_1 + L_2$), while the vertical axis is the normalized gain threshold $g_{th}L_1$. The gain is normalized with L_1 since the value of gL_1 relates to the pump power. The mode spectra of the three different lasers are nearly identical since the lasing cavities are of nearly equal length. When compared to the short DFB laser, the gain-apodized DFB lasers show a nearly 30% reduction in lasing threshold due to its passive grating section. The DFB with the reflector similarly shows a reduction in the lasing threshold for its first-order mode. However, the threshold reduction applies significantly to all modes since the reflector is spectrally uniform. For the gain-apodized DFB laser, whose passive section has spectral dependence, the additional reflector also aids in modal discrimination with higher-order modes.

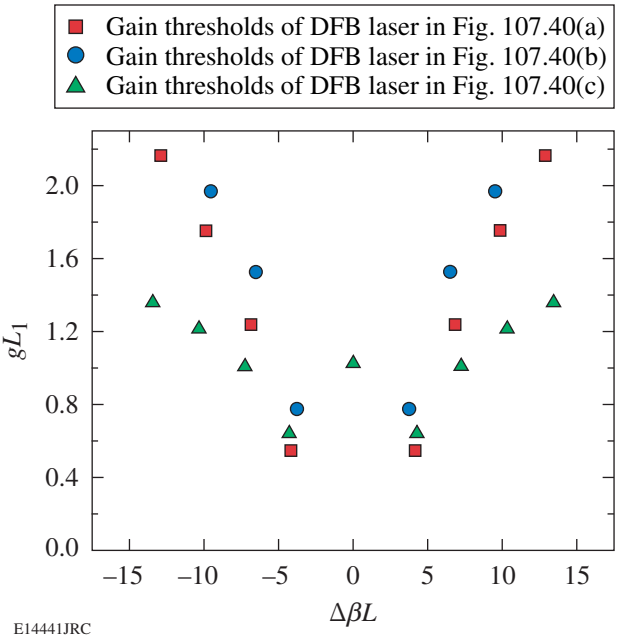

Figure 107.41
Gain thresholds of the DFB fiber laser configurations shown in Fig. 107.40.

It is also important to note that although the passive grating system introduces system asymmetry, the zeroth-order mode cannot reach the lasing threshold since the phase of the transition between the two sections is maintained. Nevertheless, Fig. 107.41 demonstrates the advantage of using gain apodization for reduced lasing threshold without the penalty of decreased spectral purity.

Figure 107.42 shows the gain threshold for DFB lasers plotted with the Bragg grating reflection spectrum to understand the interplay of active versus grating length. The grating reflection spectrum can be formulated as[17]

$$R_g(\delta) = \left| r_g(\delta) \right|^2 = \left| \frac{i\kappa \sin(qL)}{q\cos(qL) - i\delta \sin(qL)} \right|^2, \qquad (5)$$

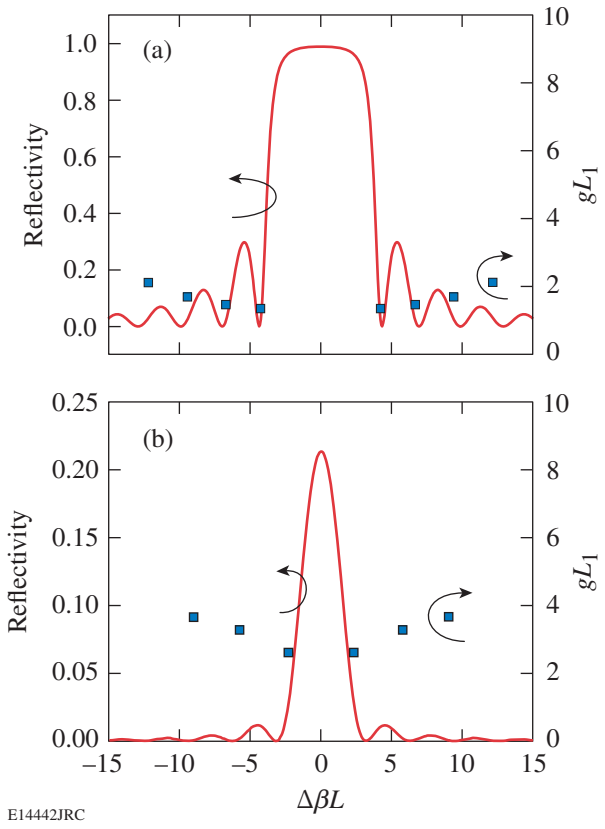

Figure 107.42
(a) The modal frequencies of a gain-apodized DFB fiber laser with $L_1 = 0.5$ cm, $L_2 = 2.5$ cm, and a reflection spectrum of a 3-cm fiber Bragg grating. (b) The modal frequencies of a 0.5-cm uniform-gain DFB fiber laser and a reflection spectrum of a 0.5-cm fiber Bragg grating.

where $\delta(\omega) = (\overline{n}/c)(\omega - \omega_B) \equiv \beta(\omega) - \beta_B$, κ is the coupling coefficient of the grating, L is the grating length, and $q = \pm\sqrt{\delta^2 - \kappa^2}$.

To exaggerate the physics, the active portion of the gain-apodized DFB fiber laser is chosen to be $L_1 = 0.5$ cm with the passive portion longer, $L_2 = 2.5$ cm. The mode spectrum of this laser and the corresponding reflectivity of a 3-cm fiber Bragg grating (FBG) are shown in Fig. 107.42(a). For comparison, Fig. 107.42(b) shows the mode spectrum of a conventional 0.5-cm-long DFB laser with the reflectivity spectrum of a 0.5-cm FBG. It is clear from these figures that the mode spectrum of the gain-apodized laser is determined by the entire grating rather than only by the active portion.

Figure 107.43 shows the lowest modal gain threshold versus gain length L_1 for the gain-apodized DFB laser. From this figure, it is clear that the minimum threshold for L_1/L is close to 0.7; the gain threshold is 17.9% less compared to the uniform DFB fiber laser ($L_1/L = 1$). For gain lengths L_1/L less than unity, the longitudinal distribution of light extends into the unpumped region, creating an effectively higher reflectivity. Since no gain is extracted from this region, the effective grating strength is increased, thus creating a lower gain threshold. For values of L_1/L that are too small (less than 0.7 in this case), the grating-length product becomes too small to produce sufficient reflection, effectively increasing the laser threshold via reduced feedback. Figure 107.43 demonstrates that gain apodization can decrease the laser threshold if properly tailored.

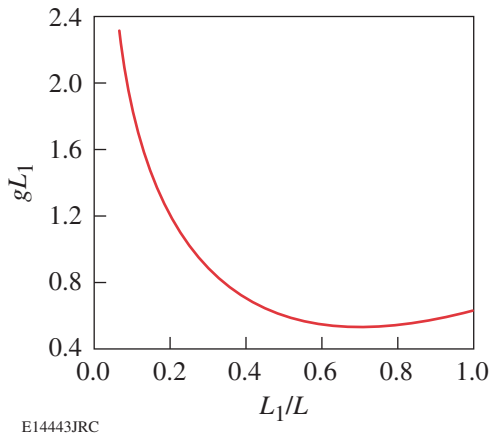

Figure 107.43
The gain thresholds of the lowest-order mode as a function of gain-apodization profile.

Impact on Phase-Shifted DFB Lasers

It is convenient to avoid mode degeneracy by introducing a phase shift in the middle of the grating. As is well known, the π-phase shift will enable a narrowband filter in the grating-forbidden band, thereby allowing the zeroth-order mode to have a low lasing threshold.[18] Considering the influence of this geometry, it is instructive to understand the role of gain apodization on phase-shifted DFB fiber lasers.

Figures 107.44(a) and 107.44(b) show the lowest-mode gain threshold and the mode discrimination of the uniform-gain, phase-shifted DFB fiber lasers. As before, the total cavity length L is 3 cm and the coupling coefficient is 1 cm^{-1}. The results show that the apodization with the lowest gain threshold also has nearly the largest mode discrimination. Slightly different to the optimum L_1/L of 0.7 for a normal DFB laser in Fig. 107.43, the optimum gain-apodization profile will be where

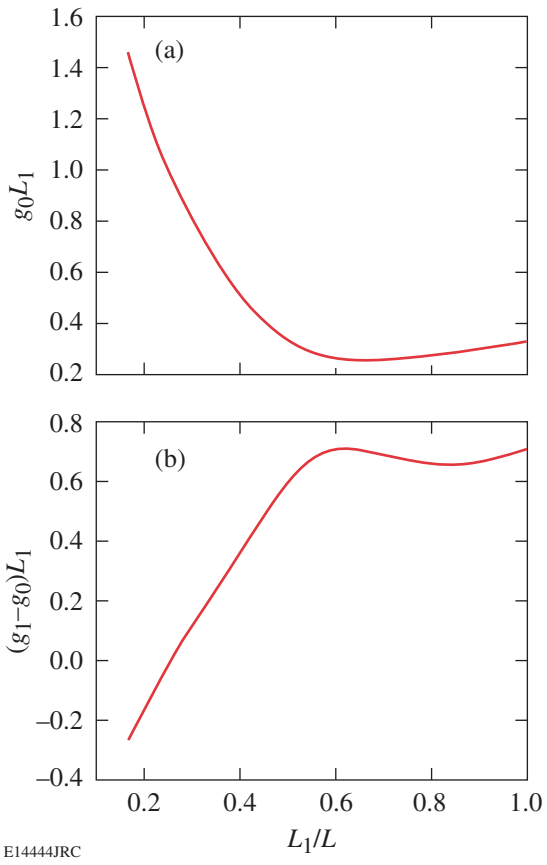

Figure 107.44
(a) The lowest-mode gain threshold versus L_1/L. (b) The mode-1 and mode-0 gain threshold difference versus L_1/L.

L_1/L is close to 0.6. From Fig. 107.44(a), the gain threshold can be reduced 21.2%, compared to the normal phase-shifted DFB fiber laser with nearly the same modal discrimination, as shown in Fig. 107.44(b).

Since the gain apodization has introduced system asymmetry, the output power ratio from both ends of the laser will also be modified. To investigate these characteristics, the output power ratio of Eq. (4) is plotted against the apodized gain length L_1/L in Fig. 107.45. The power ratio from both ends of the fiber changes monotonically with the apodization gain length L_1/L. Higher output power from the pumped end of the cavity can be obtained at the optimum pumped length L_1/L for the minimum threshold shown in Fig. 107.44(a); the power ratio can be increased by 12.4%. This asymmetry, combined with the 21.2% threshold reduction, can lead to a substantial increase in output power solely because of gain apodization.

Discussion and Conclusions

It was shown in the previous section that gain apodization can have a beneficial impact on phase-shifted DFB lasers. It has been previously shown that DFB laser performance can be improved by changing the location of the phase shift and varying κ along the laser axis.[19,20] To obtain the highest single-frequency output from DFB fiber lasers, the gain-apodization length, phase-shift location, and coupling coefficient profile must all be optimized. While this presents a challenging numerical problem, genetic algorithms have proven useful in optimizing laser and amplifier designs.[21–23]

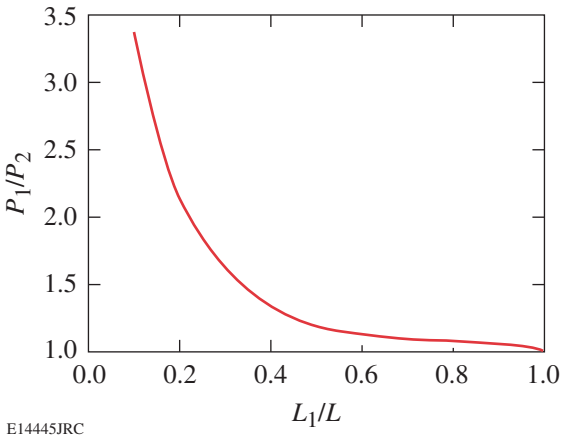

Figure 107.45
The output power ratio from the fiber ends versus L_1/L.

While the lasing threshold itself will determine the gain-apodization profile for a given DFB laser, this effect can be intentionally introduced. Two separate sections of photosensitive fiber, only one of which is doped with active ions to provide gain, can be spliced together before a grating is written into the fiber. In this way, the independent control of the gain profile, grating strength, and phase-shift location can be used to optimize of DFB laser performance.

In conclusion, the effects of gain apodization in highly doped DFB fiber lasers were investigated. In particular, apodization of the longitudinal gain profile resulted in a lower lasing threshold than a laser with uniform gain without the penalty of modal discrimination. For the case studied, the lasing threshold was reduced by almost 18% for a conventional DFB laser and over 21% for a DFB laser with a π-phase shift. Furthermore, the longitudinal asymmetry introduced by gain apodization yielded a significantly higher ratio of output power from opposite ends of the laser. Methods of engineering and optimizing such a gain-apodized DFB fiber laser were also discussed.

ACKNOWLEDGMENT

This work was supported by the U.S. Department of Energy Office of Inertial Confinement Fusion under Cooperative Agreement No. DE-FC52-92SF19460, the University of Rochester, and the New York State Energy Research and Development Authority. The support of DOE does not constitute an endorsement by DOE of the views expressed in this article.

REFERENCES

1. G. A. Cranch, M. A. Englund, and C. K. Kirkendall, IEEE J. Quantum Electron. **39**, 1579 (2003).
2. K. H. Ylä-Jarkko, IEEE Photonics Technol. Lett. **15**, 191 (2003).
3. L. Qiu *et al.*, IEEE Photonics Technol. Lett. **16**, 2592 (2004).
4. S. Foster, IEEE J. Quantum Electron. **40**, 1283 (2004).
5. Ch. Spiegelberg *et al.*, in *Optical Fiber Communications Conference, 2003*, OSA Trends in Optics and Photonics (TOPS), Vol. 86 (Optical Society of America, Washington, DC, 2003).
6. M. Ibsen *et al.*, in *Lasers and Electro-Optics, 1999 (CLEO '99)* (Optical Society of America, Washington, DC, 1999), Paper CWE4, pp. 245–246.
7. J. T. Kringlebotn, W. H. Loh, and R. I. Laming, Opt. Lett. **21**, 1869 (1996).
8. R. Gross, R. Olshansky, and M. Schmidt, IEEE Photonics Technol. Lett. **2**, 66 (1990).
9. U. Gliese, E. L. Christensen, and K. E. Stubkjaer, J. Lightwave Technol. **9**, 779 (1991).

10. J. Hübner, P. Varming, and M. Kristensen, Electron. Lett. **33**, 139 (1997).

11. F. Liu *et al.*, Electron. Lett. **36**, 620 (2000).

12. R. Böhm *et al.*, Opt. Lett. **18**, 1955 (1993).

13. H. Kogelnik and C. V. Shank, J. Appl. Phys. **43**, 2327 (1972).

14. W. Streifer, D. R. Scifres, and R. D. Burnham, IEEE J. Quantum Electron. **QE-13**, 134 (1977).

15. M. Yamada and K. Sakuda, Appl. Opt. **26**, 3474 (1987).

16. S. Radic, N. George, and G. P. Agrawal, IEEE J. Quantum Electron. **31**, 1326 (1995).

17. G. P. Agrawal, *Lightwave Technology: Components and Devices* (Wiley, Hoboken, NJ, 2004).

18. G. P. Agrawal, J. E. Geusic, and P. J. Anthony, Appl. Phys. Lett. **53**, 178 (1988).

19. K. Yelen, L. M. B. Hickey, and M. N. Zervas, IEEE J. Quantum Electron. **40**, 711 (2004).

20. K. Yelen, M. N. Zervas, and L. M. B. Hickey, J. Lightwave Technol. **23**, 32 (2005).

21. C. Cheng, Z. Xu, and C. Sui, Opt. Commun. **227**, 371 (2003).

22. M. Gao *et al.*, Opt. Express **12**, 5603 (2004).

23. C. Cheng and S. He, Microw. Opt. Technol. Lett. **22**, 343 (1999).